Supplementary material

Effective killing of bacteria under blue-light irradiation promoted by green synthesized silver nanoparticles loaded on reduced graphene oxide sheets

Cynthia S. A. Caires,[a,b†] Luiz A. S. Farias,[c†] Luiz E. Gomes,[c] Bruno P. Pinto,[c] Daniel A. Gonçalves,[a,d] Luiz F. Zagonel,[e] Valter A. Nascimento,[a] Diego C. B. Alves,[c] Ian Colbeck[b], Corinne Whitby[b], Anderson R. L. Caires[b,f]* and Heberton Wender[c]*

[a] Laboratory of Spectroscopy and Bioinformatics Applied to Biodiversity and Health, Faculty of Medicine, Federal University of Mato Grosso do Sul, Campo Grande, Mato Grosso do Sul, 79070-900, Brazil.

[b] School of Life Sciences, University of Essex, Colchester, CO4 3SQ, UK.

[c] Laboratory of Nanomaterials and Applied Nanotechnology (LNNA), Institute of Physics, Federal University of Mato Grosso do Sul, Campo Grande, Mato Grosso do Sul, 79070-900, Brazil.

[d] Department of Chemistry, Minas Gerais State University - UEMG, Ituiutaba, MG 38302-192, Brazil.

[e] "Gleb Wataghin" Institute of Physics, University of Campinas – UNICAMP, 13083-859 Campinas, São Paulo, Brazil.

[f] Laboratory of Optic and Photonics, Institute of Physics, Federal University of Mato Grosso do Sul, Campo Grande, Mato Grosso do Sul, 79070-900, Brazil.

Keywords: Green synthesis; Silver nanoparticle; Reduced graphene oxide; Blue light irradiation; Photoinactivation; *Staphylococcus aureus*.

† These authors contributed equally to this work.

*** Corresponding authors: heberton.wender@ufms.br; anderson.caires@ufms.br**

Synthesis of GO

Graphene oxide (GO) was made via modified Hammer's method [1,2][using graphite powder from the National of Graphite (Brazilian Company) with flakes diameters of <30 μm. The chemical oxidation reaction of the graphite was prepared as follows: 10 g of graphite powder and 7.56 g of sodium nitrate were mixed into 500 mL sulfuric acid under vigorous magnetic agitation for 30 min. The solution was kept in the ice-bath when 45 g of potassium permanganate was slowly added in such a way that solution temperature did not exceed 30°C. The ice-bath was removed and after five days under stirring, a dark brown and dense paste was obtained. Then, 1 L of sulfuric acid solution (5% in mass) was added and kept stirring for two hours. After that, 30 g of hydrogen peroxide (30% in mass) was added, at that time the solution turns bright yellow. After two hours, a purification process was applied to remove the impurities by using centrifugation to precipitate the solid, followed by new dispersion into a diluted solution of sulfuric acid (3% in mass), procedure that was repeated several times. All product was diluted in DI water and kept in the fume hood for 30 days to decant and get two phases of GO concentration.

ROS measurement

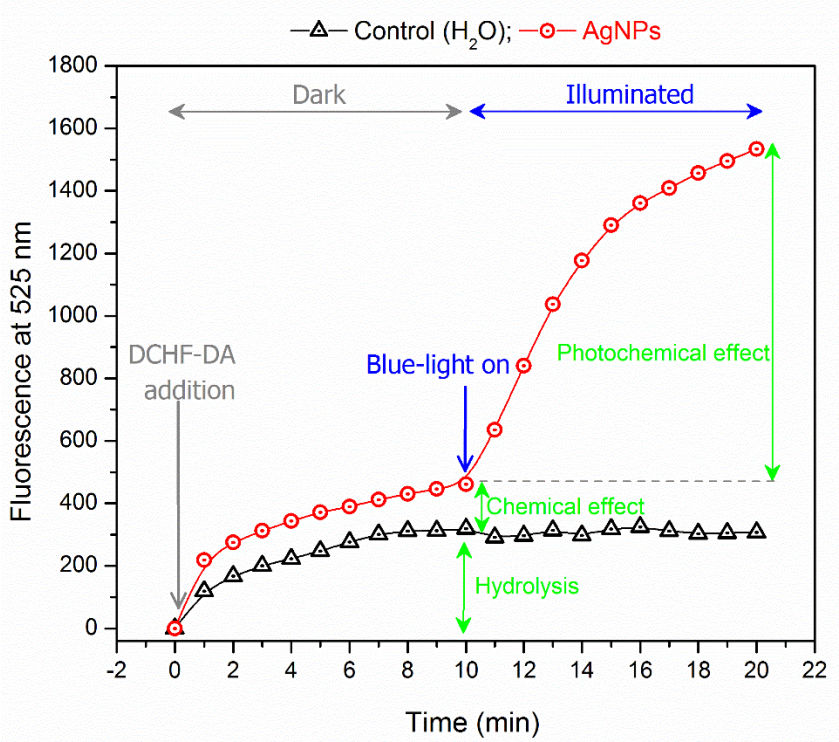

Figure S1. Fluorescence emission at 525 nm promoted by the ROS production as a function of the time.

Characterization of GO

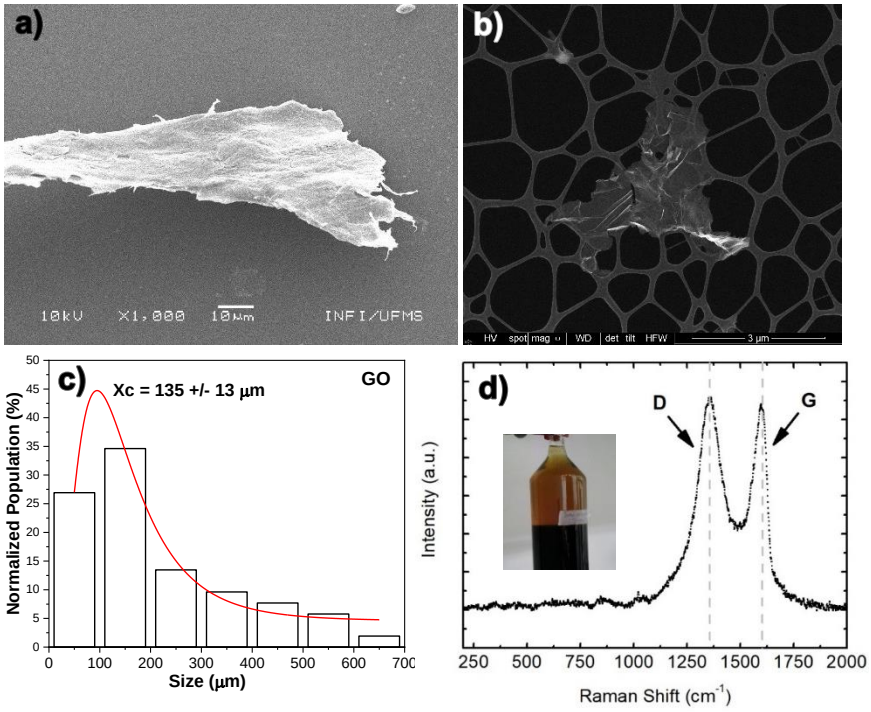

Figure S2. SEM image (a), TEM image (b), SEM histogram of the lateral size distribution (c) and Raman spectrum (c) of the GO sheets synthesized in this work.

General supplementary characterization of the samples

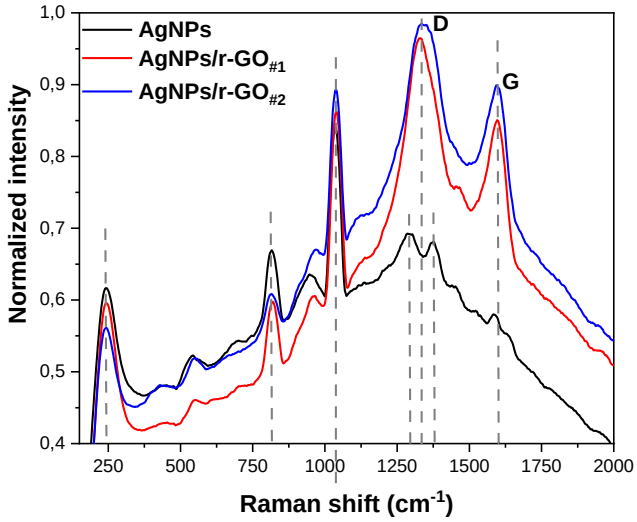

Figure S3. Raman spectra of the AgNPs, AgNPs/$GO_{\#1}$ and AgNPs/$GO_{\#2}$ samples.

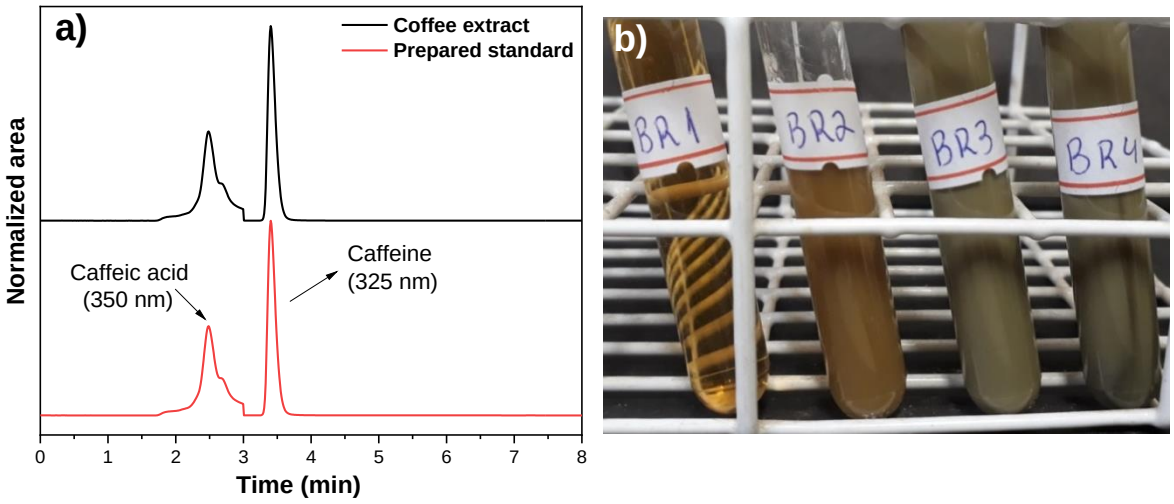

Figure S4. (a) Chromatogram of the coffee extract solution. (b) Photograph images of coffee extract (BR1), AgNPs (BR2), AgNPs/r-$GO_{\#1}$ (BR3) and AgNPs/r-$GO_{\#1}$ (BR4) obtained in this work.

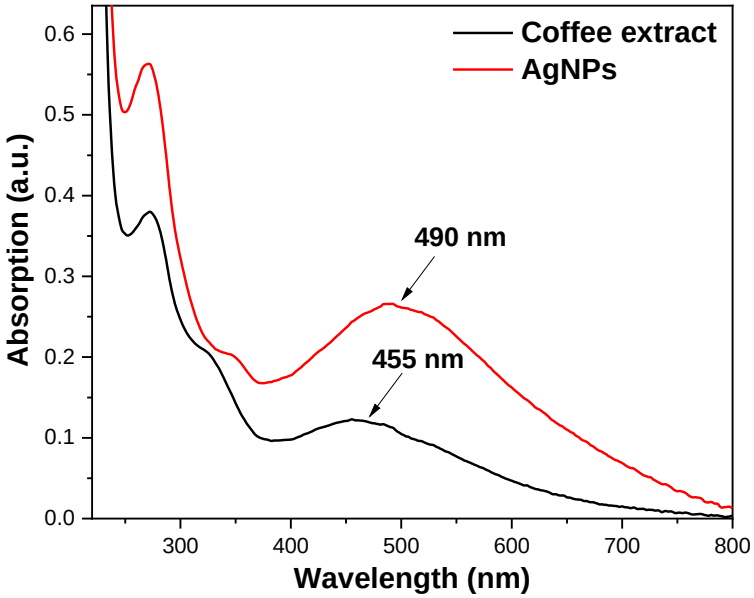

Figure S5. UV-Vis absorption spectra of coffee extract solution and AgNPs.

Table S1. Ag concentration as obtained by ICP-OES.

Sample	Ag concentration ($mg\ L^{-1}$)	RSD*
AgNPs	1255.97 ± 8.14	0.65
$AgNPs/GO_{\#1}$	1154.19 ± 0.23	0.41
$AgNPs/GO_{\#2}$	1161.35 ± 0.47	0.81

RSD* - representation of range and precision for Ag.

Table S2. Binding energies (eV) and survey quantification result in percentage obtained by XPS (sample BR4).

Region		Binding Energy (eV)		Chemical Surface Composition (%)	
		AgNPs	$AgNPs/r\text{-}GO_{\#2}$	AgNPs	$AgNPs/r\text{-}GO_{\#2}$
C 1s	C-C	284.80	284.80	71.51	67.36
	C-O	285.80	285.89		
	O=C-O	288.32	288.16		
O 1s	O-C	532.31	532.30	19.54	20.82
	C-OH	533.91	533.57		
Ag 3d	$3d_{3/2}$	374.25	374.27	4.66	5.77
	$3d_{5/2}$	368.25	368.27		
	$3d_{3/2}$ ox.	374.81	374.88		
	$3d_{5/2}$ ox.	368.81	368.88		
N 1s	-	-	-	4.29	6.05

Representative images of bacterial growth in Petri dishes

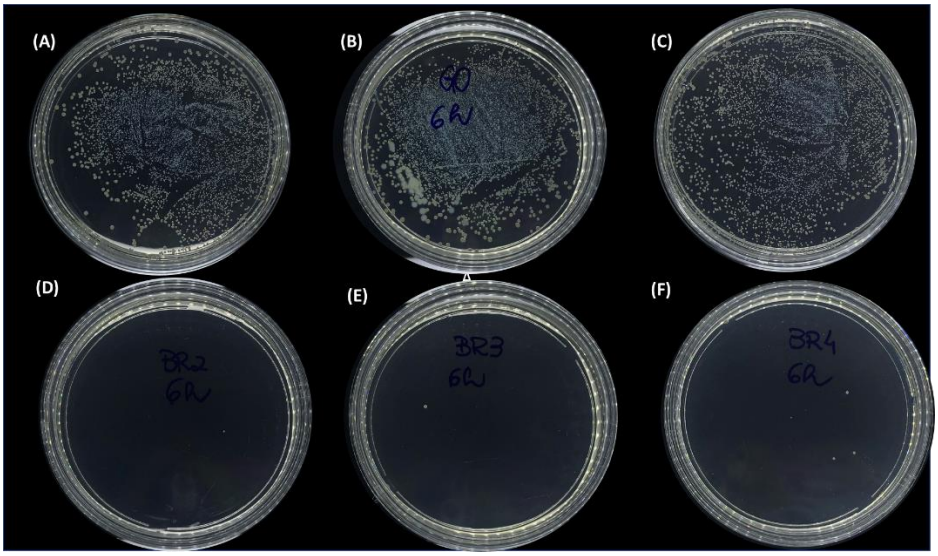

Figure S6. Growth of *S. aureus* in Petri dishes after 6.0 h of interaction with (A) H_2O, (B) GO, (C) Coffee, (D) AgNPs, (E) AgNPs/r-$GO_{\#1}$, and (F) AgNPs/r-$GO_{\#2}$ samples.

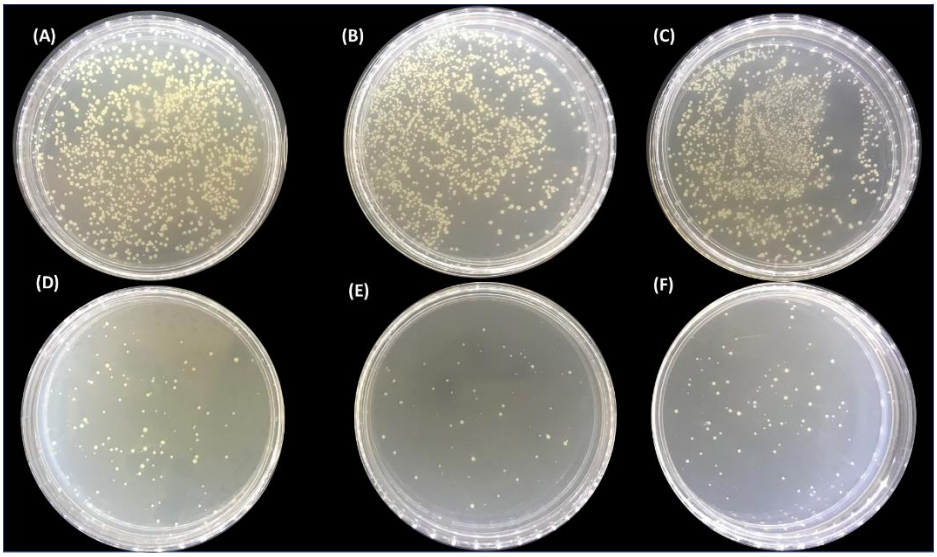

Figure S7. Growth of *S. aureus* in Petri dishes after 45 min of interaction with (A) H_2O, (B) GO, (C) Coffee, (D) AgNPs, (E) AgNPs/r-$GO_{\#1}$, and (F) AgNPs/r-$GO_{\#2}$ samples under blue light irradiation at 9.5 $mW.cm^{-2}$.

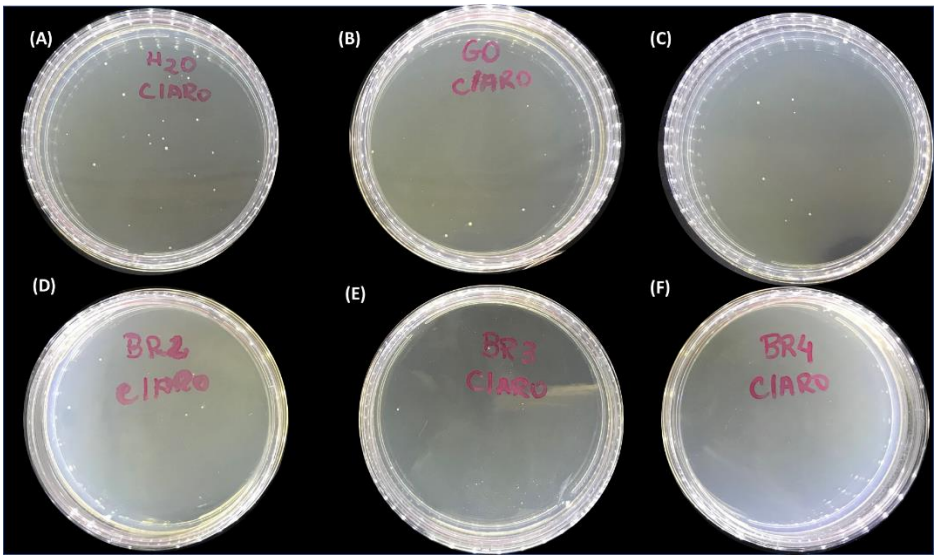

Figure S8. Growth of *S. aureus* in Petri dishes after 90 min of interaction with (A) H_2O, (B) GO, (C) Coffee, (D) AgNPs, (E) AgNPs/r-$GO_{\#1}$, and (F) AgNPs/r-$GO_{\#2}$ samples under blue light irradiation at 9.5 $mW.cm^{-2}$.

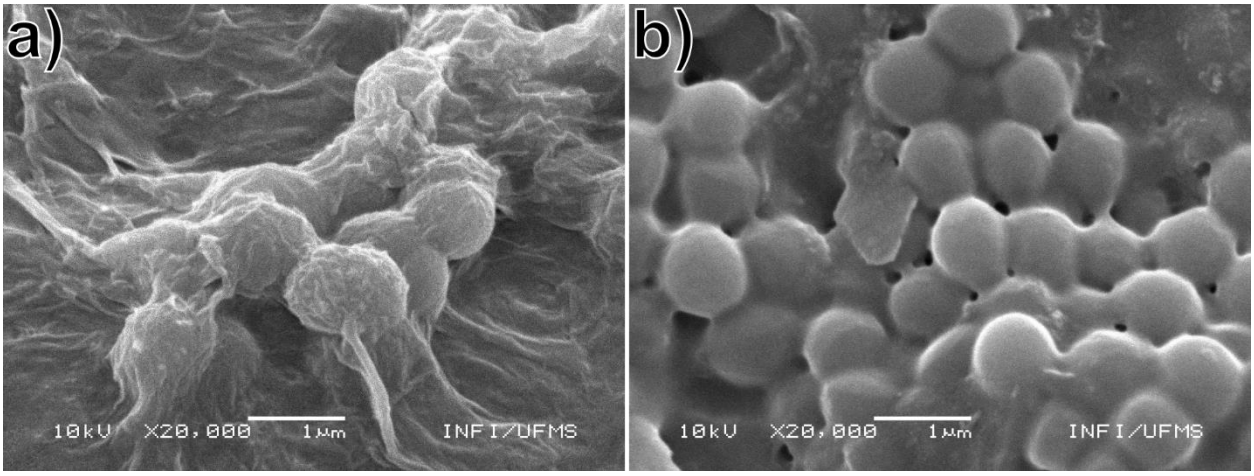

Figure S9. SEM images of (a) *S. aureus* after 6 h contact with the GO sheets showing that the bacteria were wrapped by the GO sheets and, (b) the control experiment, where regular round-shaped bacteria were identified with smooth and intact cell walls.

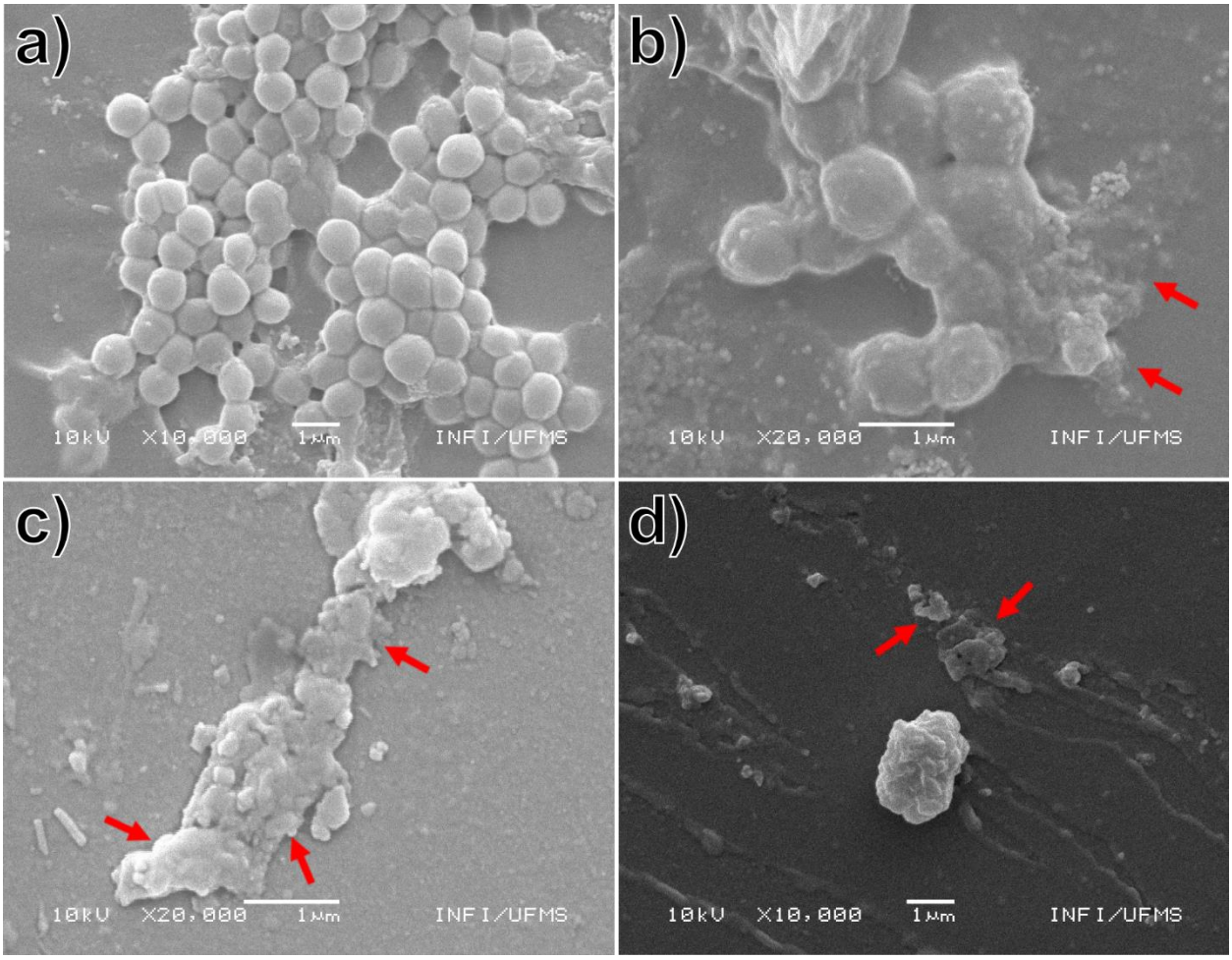

Figure S10. SEM images of *S. aureus* after 45 min of irradiation in the presence of the coffee extract (a), AgNPs (b), AgNPs/r-GO#1 (c), and AgNPs/r-GO#2 (d) samples.

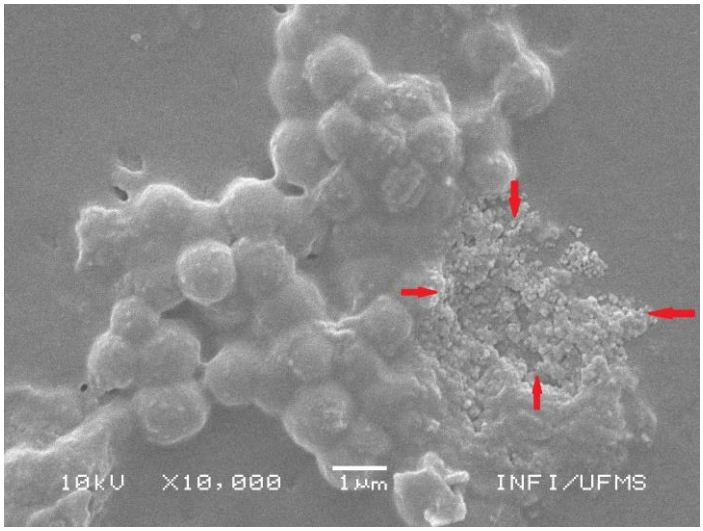

Figure S11. SEM images of *S. aureus* after 90 min under blue-light illumination.

Silver ion (Ag^+) release determination

Table S3 presents the Ag content obtained ICP OES analysis. As summarized in the experimental section, the analysed samples were collected at 48 h after the beginning of the dialysis experiments. Consequently, knowing the initial concentration of silver nanoparticles ($[A_gNPs]_o$) and the Ag^+ released concentration at 48h ($[A_g^+]_{48}$), we determined the Ag dissolution rate constant ($K_d^{A_g^+}$) for each sample by using Equation S2. Table S4 shows the Ag^+ release from AgNPs in distilled water, for the times related to the bioassay times, determined by using Equation S1.

Table S3 - Ag^+ release from AgNPs in distilled water.

	AgNPs	**AgNPs/GO$_{\#1}$**	**AgNPs/GO$_{\#2}$**
Ag^+ (mg.L^{-1}) at 48h	35.9 ± 1.5	34.4 ± 1.2	35.6 ± 2.0
$K_d^{A_g^+}$ (h^{-1})	0.027 ± 0.001	0.025 ± 0.001	0.026 ± 0.002

$$[A_g^+]_t = [A_gNPs]_o(1 - e^{-(K_d^{A_g^+})t}) \quad \textbf{(S1)}$$

$$[A_g^+]_t = [A_gNPs]_o\left(1 - e^{-(K_d^{A_g^+})t}\right) \rightarrow \frac{[A_g^+]_t}{[A_gNPs]_o} = 1 - e^{-(K_d^{A_g^+})t} \rightarrow e^{-(K_d^{A_g^+})t}$$

$$= 1 - \frac{[A_g^+]_t}{[A_gNPs]_o}$$

$$\rightarrow \ln(e^{-(K_{\mathrm{d}}^{A_g^+})t}) = \ln(1 - \frac{[A_g^+]_t}{[A_g NPs]_o}) \rightarrow -(K_{\mathrm{d}}^{A_g^+})t = \ln(1 - \frac{[A_g^+]_t}{[A_g NPs]_o}) \rightarrow K_{\mathrm{d}}^{A_g^+}$$

$$= -\frac{\ln(1 - \frac{[A_g^+]_t}{[A_g NPs]_o})}{t}$$

$$\boldsymbol{K_{\mathrm{d}}^{A_g^+} = -\frac{\ln(1-\frac{[A_g^+]_t}{[A_g NPs]_o})}{t}} \qquad \textbf{(S2)}$$

Table S4 - **Ag^+ release (in % of the initial mass) from AgNPs in distilled water.**

	AgNPs		**AgNPs/GO$_{\#1}$**		**AgNPs/GO$_{\#2}$**	
Time (h)	Ag^+ (mg.L^{-1})	Ag^+ (%)	Ag^+ (mg.L^{-1})	Ag^+ (%)	Ag^+ (mg.L^{-1})	Ag^+ (%)
1.0	1.31 ± 0.05	2.6 ± 0.1	1.20 ± 0.04	2.4 ± 0.1	1.28 ± 0.07	2.6 ± 0.1
1.5	1.95 ± 0.08	3.9 ± 0.2	1.79 ± 0.06	3.6 ± 0.1	1.91 ± 0.10	3.8 ± 0.2
2.5	3.20 ± 0.13	6.4 ± 0.3	2.95 ± 0.10	5.9 ± 0.2	3.13 ± 0.17	6.3 ± 0.4
3.0	3.82 ± 0.16	7.6 ± 0.3	3.51 ± 0.12	7.0 ± 0.3	3.74 ± 0.21	7.5 ± 0.4
6.0	7.35 ± 0.32	14.7 ± 0.7	6.78 ± 0.24	13.6 ± 0.5	7.20 ± 0.42	14.4 ± 0.8

Kinetic analysis of the ROS production (reaction between DCFH-DA and ROS)

The rate constant of ROS production was estimated by kinetic analysis of fluorescent products generated due to the interaction between DCFH-DA and ROS. DCFH-DA was used at a saturating concentration during the fluorescent measurments and it was assumed that the rate of new fluorescent products [F] formation is equal to ROS generation by AgNPs-containing samples under blue-light illumination as follows [3]:

$$\boldsymbol{DCFH : DA + ROS \xrightarrow{k} F}$$

Consequently, the rate of ROS production can be written as presented by Eq. S3:

$$-\frac{d[ROS]}{dt} = k_{ROS}\,[DCFH:DA][ROS] \quad \textbf{(S3)}$$

where k_{ROS} is the apparent rate constant of ROS production (i.e., the apparent rate constant for the reaction of DCFH-DA with ROS) under the experimental conditions, which $[ROS] \propto F$. Therefore, Eq. S3 can be represented by Eq. S4:

$$-\frac{dF}{dt} = kF \quad \textbf{(S4)}$$

where $k = k_{ROS}[DCFH{:}DA]$. Consequently, the experimental data can be fitted by Eq. S5 to dertermine k

$$F = a(1 - e^{-kt}) \quad \textbf{(S5)}$$

Finally, we determined k_{ROS} diving the obtained values of k by the known concentration of DCFH-DA used during the experimental analysis. It is important to stress that a fixed value of the a constant was used for all samples during the fitting analysis, leaving only k as a free parameter (fitting curves are presented in Fig. 8).

Table S5: Rate constant of ROS production under blue-light irradiation.

	k (10^{-3} s^{-1})	k_{ROS} ($M^{-1}s^{-1}$)
Coffee	0.18±0.01	0.54±0.02
GO	0.81±0.02	2.43±0.07
AgNPs	2.92±0.07	8.77±0.20
AgNPs/GO$_{\#1}$	5.72±0.23	17. 18±0.71
AgNPs/GO$_{\#2}$	4.75±0.15	14.26±0.43

Endogenous photosensitizer extraction and identification

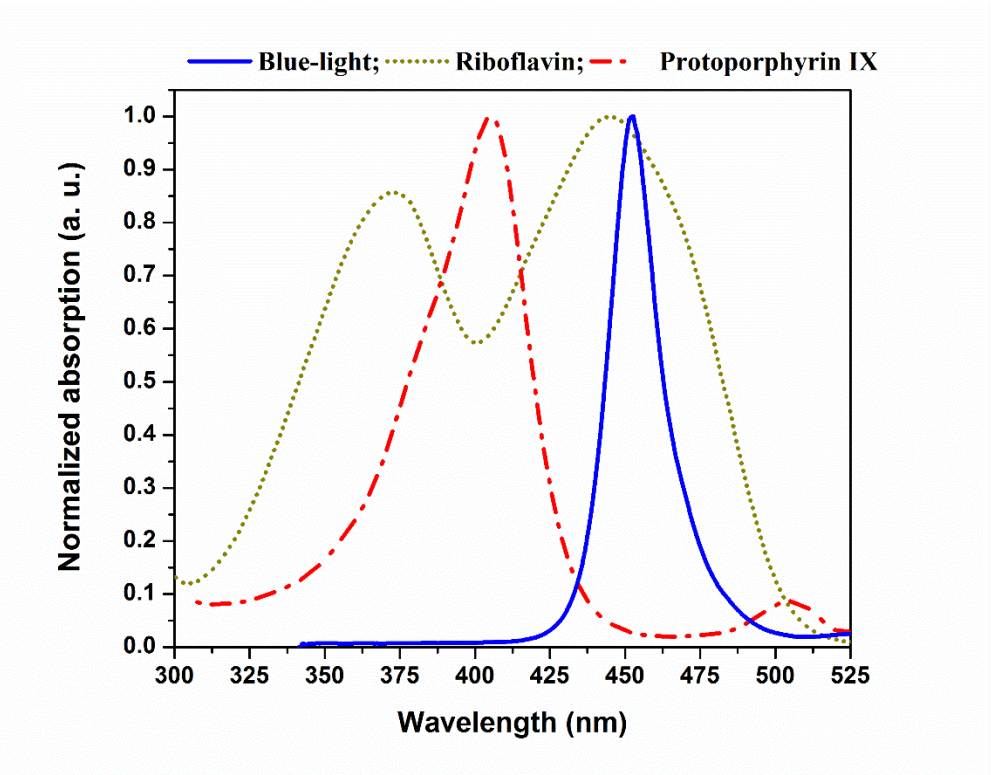

Figure S12. Absorption spectra of riboflavin (dotted line) and protoporphyrin IX (doted-dashed line), and emission spectrum of LED excitation device (solid line).

References

[1] M. Hirata, T. Gotou, S. Horiuchi, M. Fujiwara, M. Ohba, Thin-film particles of graphite oxide 1:, Carbon N. Y. 42 (2004) 2929–2937. doi:10.1016/j.carbon.2004.07.003.

[2] W.S. Hummers, R.E. Offeman, Preparation of Graphitic Oxide, J. Am. Chem. Soc. 80 (1958) 1339. doi:10.1021/ja01539a017.

[3] H. Zhao, S. Kalivendi, H. Zhang, J. Joseph, K. Nithipatikom, J. Vásquez-Vivar, B. Kalyanaraman, Superoxide reacts with hydroethidine but forms a fluorescent product that is distinctly different from ethidium: potential implications in intracellular fluorescence detection of superoxide, Free Radic. Biol. Med. 34 (2003) 1359–1368. doi:10.1016/S0891-5849(03)00142-4.